Photorefractive Polymer with Side-Chain Second-Order Nonlinear Optical and Charge-Transporting Groups

Chanfeng Zhao, Chi-Kyun Park, and Paras N. Prasad*

Photonics Research Laboratory, Department of Chemistry, State University of New York at Buffalo, Buffalo, New York 14260

Yue Zhang, Saswati Ghosal, and Ryszard Burzynski

Laser Photonics Technology, Inc., 1576 Sweet Home Rd., Amherst, New York 14228

Received January 13, 1995. Revised Manuscript Received March 28, 1995[⊗]

We report the synthesis and characterization of a new, low-T_g polymer exhibiting the photorefractive effect. The photorefractive polymer contains a second-order nonlinear optical chromophore, a charge transporting group, and a long aliphatic chain covalently linked to the polymer backbone. A sensitizer (C_{60}) was molecularly doped into the polymer to facilitate photocharge generation. The photoconductivity, electrooptic (Pockels) effect, and photorefractive properties of the polymer are reported.

I. Introduction

The photorefractive (PR) effect in various inorganic crystals have been extensively investigated for many years.[1,2] Photorefractive materials have many potential applications in coherent optical systems including holographic data storage, real-time image processing and optical switching. To manifest photorefractivity, a material must simultaneously possess photoconductivity and electrooptic effect.[1,2] Polymeric photorefractive materials[3–14] have emerged in the last few years as attractive candidates for these applications owing to their large nonlinearities, low dielectric constants and ease of processing. Photorefractive figures-of-merit superior to that of inorganic crystals have been obtained with the demonstration of holographic diffraction efficiencies as high as 100% and two-beam coupling energy-transfer gains as large as 220 cm^{-1}.[15–18] A photorefractive volume storage device has been proposed and demonstrated for selective readout.[11] A particularly attractive feature of such polymeric photorefractive media is that the photoconduction wavelength can be chosen as desired since photocharge generation sensitizers are available throughout the visible to near-infrared. Also, charge-transporting and -trapping properties can be tailored by the addition of molecules with appropriate ionization energy or electron affinity. Most of the reported polymeric photorefractive materials have been based on guest–host systems using either a nonlinear optical polymer or a charge-transporting polymer host.[5–8] There have also been reports of inert polymers doped with three components: a charge-transporting agent, a second-order chromophore, and a photocharge generation sensitizer.[9,10] Recently, bifunctional chromophores have been reported which function as charge-transporting agents as well as second-order nonlinear optical compounds.[11,12] However, there are inherent problems of phase separation in these doped systems which adversely limits the chromophore concentration and, thus, the value of achievable electrooptic coefficient. Consequently, the photorefractive efficiencies and figures-of-merit are limited.

The ultimate solution to this problem lies, perhaps, in the design and preparation of photorefractive polymers[13,14] where both the NLO chromophore and charge-transporting molecule are covalently attached to or are functional units forming the polymer backbone. The advantage of such polymers over doped systems is that such single-component systems are more stable against

[⊗] Abstract published in *Advance ACS Abstracts,* May 1, 1995.

(1) Gunter, P.; Huignard, J. P., Eds. *Photorefractive Materials and Their Applications*; (Springer-Verlag: New York, 1988; I & II, Topics in Applied Physics Vols. 61 and 62.
(2) Yeh, P. C. *Introduction to Photorefractive Nonlinear Optics*; Wiley: New York, 1993.
(3) Ducharme, S.; Scott, J. C.; Twieg, R. J.; Moerner, W. E. *Phys. Rev. Lett.* **1991**, *66*, 1864.
(4) Moerner, W. E.; Silence, S. M. *Chem. Rev.* **1994**, *94*, 127.
(5) Moerner, W. E.; Walsh, C. A.; Scott, J. C.; Twieg, R. J. *Proc. SPIE* **1991**, *1560*, 278.
(6) Zhang, Y.; Cui, Y. P.; Prasad, P. N. *Phys. Rev.* B **1992**, *46*, 9900.
(7) Cui, Y. P.; Zhang, Y.; Prasad, P. N.; Schildkraut, J. S.; Williams, D. J. *Appl. Phys. Lett.* **1992**, *61*, 2132.
(8) Silence, S. M.; Walsh, C. A.; Scott, J. C.; Moerner, W. E. *Appl. Phys. Lett.* **1992**, *61*, 2967.
(9) Yokoyama, K.; Arishima, K.; Shimada, T.; Sukegawa, K. *Jpn. J. Appl. Phys.* **1994**, *33*, 1029.
(10) Burzynski, R.; Zhang, Y.; Ghosal, S.; Casstevens, M. K. *Polym. Prepr.*, in press.
(11) Stankus, J. J.; Silence, S. M.; Twieg, R. J.; Burland, D. M.; Miller, R. D.; Scott, J. C.; Moerner, W. E.; Bjorklund, G. C. *Proc. SPIE* **1994**, *2285*, 204.
(12) Zhang, Y.; Ghosal, S.; Casstevens, M. K.; Burzynski, B. *Appl. Phys. Lett.* **1995**, *66*, 256.
(13) Kippelen, B.; Tamura, K.; Peyghambarian, N.; Padias, A. B.; Hall, H. K. Jr. *J. Appl. Phys.* **1993,** *74*, 3617. Kippelen, B.; Tamura, K.; Peyghambarian, N.; Padias, A. B.; Hall, H. K., Jr. *Phys. Rev.* B **1993,** *48*, 10710.
(14) Yu, L. P.; Chan, W. K.; Bao, Z. N.; Cao, S. X. F. *J. Chem. Soc., Chem. Commun.* **1992,** 1735. Yu, L. P.; Chan, W. K.; Bao, Z. N.; Cao, S. X. F. *Macromolecules* **1993,** *26*, 2216. Yu, L. P.; Chen, K. M.; Chan, W. K.; Peng, Z. H. *Appl. Phys. Lett.* **1994**, *64*, 2489.
(15) Orczyk, M. E.; Zieba, J.; Prasad, P. N. In *Organic Thin Films for Photonic Applications Technical Digest, 1993*; Vol. 17 Optical Society of America: Washington, DC, 1993; pp 224–227.
(16) Orczyk, M. E.; Zieba, J.; Prasad, P. N. *J. Phys. Chem.* **1994**, *98*, 8699.
(17) Orczyk, M. E.; Swedek, B.; Zieba, J.; Prasad, P. N. *J. Appl. Phys.* **1994**, *76*, 4995.
(18) Meerholz, K.; Volodin, B. L.; Sandalphon; Kippelen, K.; Peyghambarian, N. *Nature* **1994**, *371*, 497.

0897-4756/95/2807-1237$09.00/0

phase separation and sublimation during sample preparation. However, for organic PR polymers, the charge mobility is strongly dependent upon the interparticle separation between transport molecules. It is often assumed that materials with high charge mobility are required to increase the speed of photorefractive response. Compared with guest–host systems, the molecules in fully functional polymers are attached to the backbone, and the molecular motions are restricted to very short-range vibrations and rotations at temperatures below the glass transition temperature (T_g). The lack of mobility may thus interrupt the conduction pathway of the charge-transporting molecules. Another parameter affecting the performance of PR polymers is their glass transition temperature, which determines not only the efficiency of the electric field poling process which is required to introduce a noncentrosymmetry, but also the stability of the poled structure. Since an electric field is always applied to facilitate photocharge generation, it is not necessary to have a high-T_g system because the electric field will align the chromophore. However, too-low T_g may result in poling degradation of the samples.

We report in this paper the design, synthesis, and characterization of a new photorefractive polymer, poly-([4-(*N*-ethyl-*N*-(hydroxyethyl)amino)-4′-nitrostilbenyl methacrylate]-*co*-[*N*-(2-hydroxyethyl)carbazolyl]-*co*-[*n*-octyl methacrylate]) (PENHCOM), which contains a second-order chromophore and a charge-transporting molecule covalently attached to the polymer backbone. (A charge-generating sensitizer was molecularly doped into the polymer. Since the concentration of the sensitizer is very low, phase separation is unlikely to occur.) The charge-transporting and the second-order segments of the polymer are an *N*-alkylated carbazole group and a stilbene derivative, respectively. The long aliphatic octyl methacrylate group serves the purpose of lowering the polymer's glass transition temperature. The synthesis of the polymer along with the characterization techniques are described in section II. In section III, experimental results on the electrooptic coefficient, photoconductivity, and photorefractive properties are presented. Results of four-wave mixing and two-beam coupling show that the observed phenomenon is indeed photorefractive.

II. Experimental Section

A. Synthesis. Ethylene oxide was purchased from Fluka Co. *n*-Octyl methacrylate and 2,2′-azobisisobutyronitrile (AIBN) were purchased from Polysciences, Inc. AIBN was recrystallized twice from methanol. All other chemicals were bought from the Aldrich Chemical Co. and were used as received unless stated otherwise. The synthetic schemes of the monomers and the polymer are shown in Schemes 1 and 2. Melting temperature of all the monomers was determined using a Fisher-Johns melting point apparatus and was uncorrected. Differential scanning calorimetry (DSC) thermogram of the polymer was taken using a Shimadzu DSC-50GPC instrument under nitrogen. Proton NMR spectra were recorded by a Varian Gemini-300 300 MHz spectrometer. UV/visible spectra were recorded with a Shimadzu UV-3101 PC spectrophotometer.

*4-(N-Ethyl-N-(hydroxyethyl)amino)benzaldehyde (**3**)*:[19] A 1-L three-neck flask fitted with mechanical stirrer, thermometer, and condenser was charged with 25 g (0.2 mol) of 4-fluorobenzaldehyde (**1**), 54 g (0.6 mol) of 2-(ethylamino)ethanol, 41.5 g (0.3 mol) of anhydrous potassium carbonate, and 0.5 mL of Aliquat-336 in 250 mL of dimethylsulfoxide (DMSO). The reaction mixture was heated at 95 °C for 72 h, and after cooling to room temperature it was poured into an ice water mixture. The water layer was extracted with dichloromethane, and the organic layer was washed twice with cold water. After solvent evaporation, the reddish oil was dissolved in 200 mL of ether and poured into 800 mL of 1 N hydrochloric acid (HCl) in water. After stirring for 10 min, the water layer was separated and neutralized using an aqueous sodium carbonate solution. Then 200 mL of dichloromethane was added; the organic layer was separated and dried with anhydrous sodium sulfate. The product was obtained as a pale yellow oil after removing the solvent, yield 25 g (65%). ^{1}H-NMR ($CDCl_3$) δ 1.18 (t, 3H), 2.30 (s, 1H), 3.62 (m, 2H), 3.66 (t, 2H), 3.90 (t, 2H), 6.70 (d, 2H), 7.68 (d, 2H), 9.62 (s, 1H) ppm.

(19) DeMartino, R. D. U.S. Patent, 4,757,130, 1988.

Scheme 1

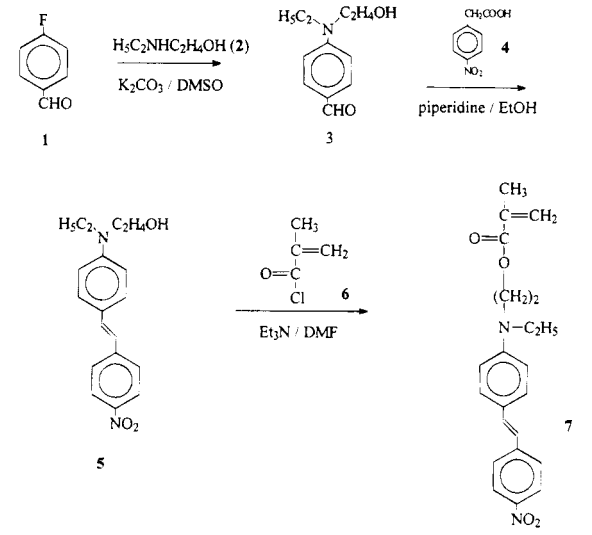

Scheme 2

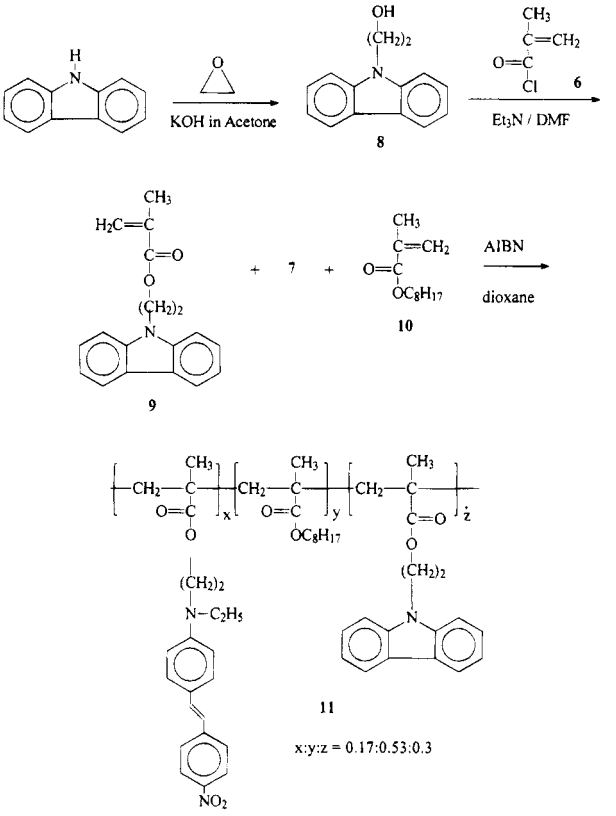

4-(N-Ethyl-N-hydroxyethylamino)-4'-nitrostilbene (5):[19] In a 500-mL three-neck flask fitted with mechanical stirrer and condenser was added 4 g (22 mmol) of 4-nitrophenylacetic acid (**4**), and 3 mL (2.6 g, 30 mmol) of piperidine was added, followed by the addition of 2 g (10 mmol) of 4-(*N*-ethyl-*N*-(hydroxyethyl)amino)benzaldehyde. The resultant mixture was heated at 100 °C for 3 h and at 130 °C for 3 h. After cooling the mixture, 50 mL of ethanol was added to the semisolid, filtered, washed, and vacuum dried. The crude product was recrystallized from chlorobenzene. The red crude product was finally purified by using column chromatography (dichloromethane:methanol = 99:1), yield: 2.34 g (75%), mp 165–166 °C. ^{1}H NMR ($CDCl_3$) δ 1.18 (t, 3H), 1.65 (s, 1H), 3.42 (t, 2H), 3.48 (q, 2H), 3.80 (t, 2H), 6.70 (d, 2H), 6.85 (d, 1H), 7.20 (d, 1H), 7.38 (d, 2H), 7.50 (d, 2H), 8.15 (d, 2H) ppm.

9-(β-Hydroxyethyl)carbazole (8):[20] A 100-mL three-neck flask was fitted with mechanical stirrer, thermometer, and dry ice–acetone condenser. To a slurry of 33.4 g (0.2 mol) of carbazole and 11.2 g (0.2 mol) of powdered potassium hydroxide (KOH) in 70 mL of freshly dried acetone at 0 °C, 10 mL of ethylene oxide (cooled to 0 °C) was added. The mixture was heated at 55–60 °C for 50 min and then cooled and washed with cold water. The product solidified during washing with water was filtered and then dried at 50–60 °C under vacuum (10^{-2} Torr), and then recrystallized twice from a 1:1 benzene–hexane mixture to obtain 25 g (60%) white solid product, mp 82–83 °C. ^{1}H NMR (DMSO-d_6) δ 3.76 (t, 2H), 4.40 (t, 2H), 4.88 (t, 1H), 7.18 (t, 2H), 7.40 (t, 2H), 7.60 (d, 2H), 8.10 (d, 2H) ppm.

4-(N-Ethyl-N-(hydroxyethyl)amino)-4'-nitrostilbenyl methacrylate (7): In a 500 mL three-neck flask fitted with nitrogen gas inlet, mechanical stirrer, and thermometer, 3.12 g (10 mmol) of 4-(*N*-ethyl-*N*-(hydroxyethyl)amino)-4'-nitrostilbene and 16.5 mL (12 mmol) of triethylamine were dissolved in 50 mL of dried DMF. The temperature of the solution was brought down to 0–5 °C followed by dropwise addition of 1.2 g (12 mmol) of methacryloyl chloride. The mixture was stirred for 1 h at 5 °C and overnight at room temperature. After filtration to remove the amine salt, the solution was poured into water to precipitate out the red solid product which was recrystallized twice from an ethanol:water (1:1) mixture, yield 2.3 g (61%), mp 60 °C. ^{1}H-NMR ($CDCl_3$) δ 1.18 (t, 3H), 1.60 (s, 3H), 3.42 (m, 2H), 3.60 (t, 2H), 4.30 (t, 2H), 5.54 (s, 1H), 6.04 (s, 1H), 6.70 (d, 2H), 7.40 (d, 2H), 7.50 (d, 2H), 8.15 (d, 2H) ppm.

N-(2-hydroxyethyl)carbazolyl methacrylate (9): The above procedure was repeated for the formation of **9**, using 2.1 g (10 mmol) of **8**. Recrystallization from methanol yielded 1.84 g (66%) of white solid, mp 78 °C. ^{1}H NMR ($CDCl_3$) δ 1.79 (s, 3H), 4.52 (t, 2H), 4.61 (t, 2H), 5.46 (s, 1H), 5.92 (s, 1H), 7.24 (t, 2H), 7.42 (t, 2H), 7.48 (d, 2H), 8.10 (d, 2H) ppm.

PENHCOM polymer (11): In a joint-cup bottle, 646 mg (1.7 mmol) of **7**, 838 mg (3 mmol) of **9**, 1.05 g (5.3 mmol) of **10**, and 16 mg (0.1 mmol) of AIBN were dissolved in 30 mL of freshly dried 1,4-dioxane and heated under argon at 60 °C for 24 h. The copolymer was precipitated from 100 mL of methanol, dried in vacuum at room temperature, and purified by reprecipitation from dioxane and methanol twice. The resulting polymer was then dialyzed for 14 days using a SIGMA dialysis tubing to remove monomers and oligomers with molecular weight less than 12 000. ^{1}H NMR ($CDCl_3$) δ 0.85 (br, 6H), 1.18 (s, 9H), 1.56 (s, 6H), 3.40 (br, 2H), 3.96 (br, 2H), 4.40 (br, 2H), 6.7 (br, 2H), 7.04 (br, 2H), 7.40 (br, 4H), 8.10 (br, 2H) ppm. Inherent viscosity 1.05 (in cyclopentanone, 25 °C). Anal. Calcd for $(C_{22}H_{24}N_2O_4)_{1.7}(C_{12}H_{22}O_2)_{5.3}(C_{18}H_{17}NO_2)_3$: C, 73.41; H, 8.28; N, 3.54. Found: C, 73.15; H, 8.38; N, 3.38.

PENHCOM is soluble in a variety of organic solvents, such as chloroform, toluene, THF, DMF, etc. Good optical quality film can be cast from the polymer solution. The UV/vis spectrum (Figure 1) of the polymer showed the absorption of the NLO chromophore at 435 nm and that of the transporting compound at 340 nm in chloroform which are similar to those of corresponding monomers. The NMR spectra clearly indicate

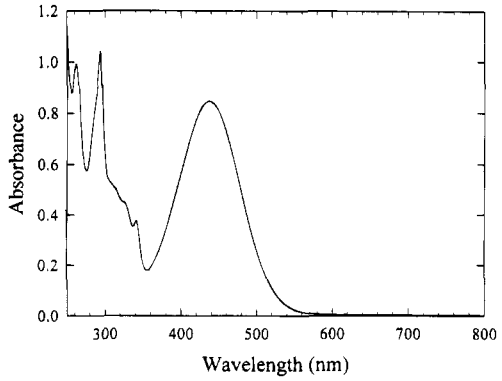

Figure 1. UV/vis spectra of the polymer, in chloroform.

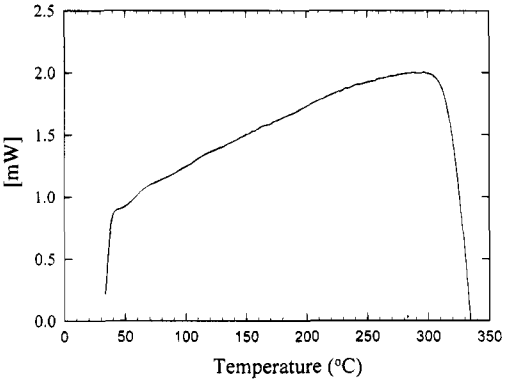

Figure 2. DSC thermal analysis, heating rate: 10 °C/min.

that all the monomer species are indeed incorporated into the polymer chain. Figure 2 shows the DSC spectrum of the polymer. The T_g of the polymer is 47 °C (heating rate 10 °C/min, under nitrogen), and it is thermally stable up to 300 °C. Viscosity was measured using a Ubbelohde viscometer at 25 °C constant bath temperature. Elemental analyses were performed by Atlantic Microlab, Inc. P.O. Box 2288, Norcross, GA 30091.

B. Sample Preparation and Measurements. To be photorefractive, a material must possess both photoconductivity and an electrooptic effect. Therefore, the basic characterization of the material must include the measurement of its electrooptic coefficient and photoconductivity properties. Samples used for these measurements were prepared by spin coating from solutions onto indium tin oxide (ITO) covered glass substrates. All films were dried at 100 °C for at least 24 h for solvent evaporation. A thin layer of gold electrode was then deposited on the top of the polymer film by vacuum evaporation. The electrooptic coefficient of the film was measured at a wavelength of 633 nm using a reflection technique as described by Teng and Man.[21] The photoconductivity was measured using a simple photocurrent technique.[22] In this experiment, a dc voltage was applied to the gold electrode while the ITO layer was grounded. A He–Ne laser beam illuminated the sample through the glass substrate to generate photocharge carriers inside the polymer. The photocurrent was measured by monitoring the voltage drop on a resistor which is in series with the film capacitor.

The photorefractive properties of the polymer were studied by the four-wave mixing (FWM) and two-beam coupling (TBC) techniques[4] using an experimental setup described in Figure 3. Samples are prepared as follows. C_{60} and PENHCOM were dissolved in toluene at concentrations of 0.05 and 15 wt %, respectively; the solutions were mixed in a proportion to yield solid samples containing 0.2 wt % of C_{60} and 99.8 wt % of PENHCOM. The solution mixture was then heated to 100 °C for solvent evaporation. The resulting solid was sandwiched between ITO-covered glass substrates at an elevated temper-

(20) Lopatinski, V. P.; Sirotkina, E. E.; Zherebstsov, I. P. *Chem. Abst.* 19542f, **1966**, Vol. 64.

(21) Teng, C. C.; Man, H. T. *Appl. Phys. Lett.* **1990**, *56*, 1735.
(22) Schildkraut, J. S. *Appl. Phys. Lett.* **1991**, *58*, 340.

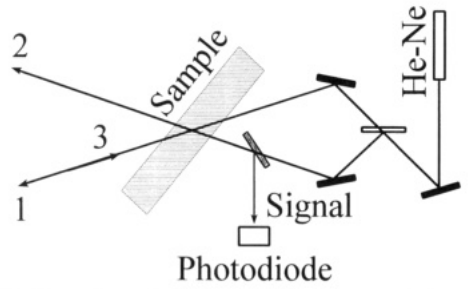

Figure 3. Experimental setup for four-wave mixing and two-beam coupling.

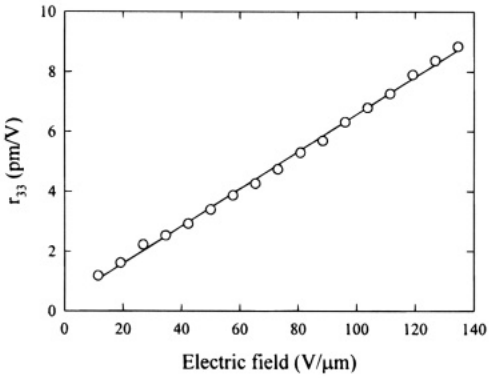

Figure 4. Electric field dependence of the electrooptic coefficient measured by the reflection technique. Open circles: experimental data; solid curve: fit to eq 1.

ature at which the polymer softens. The sample thickness was controlled to be around 100 μm with the help of Teflon spacers. Samples prepared in this manner are of excellent optical quality and are transparent for wavelengths above 600 nm.

Because of the polymer's low T_g, no poling was performed prior to photorefractive measurements which were carried out at room temperature. Holographic gratings are written by two laser beams from a He−Ne laser operating at 633 nm. Two writing beams with an equal intensity of 250 mW/cm^2 intersect in the sample at incidence angles of $\theta = 45°$ and $\theta = 62°$ (in air), respectively, and create an intensity grating with a spacing Λ of around 3 μm (depending on the material's refractive index). The reading beam from another He−Ne laser at 633 nm with an intensity of 10 mW/cm^2 propagates in the direction opposite to one of the writing beams (beam 2) and gets diffracted in the direction opposite to that of beam 1; it is then reflected off the beam splitter and detected by a photodiode. In a two-beam coupling experiment, the energy transfer between the p-polarized writing beams is observed by monitoring the intensity of each of the writing beams when an external electric field is applied. The same energy transfer is also observed by the increase (or decrease) of the beam intensity while the other writing beam is open and blocked.

III. Results

A. Electrooptic and Photoconductivity Data. Figure 4 displays the electric field dependence of the electrooptic coefficient measured by the reflection technique. The field dependence of the electrooptic coefficient can be expressed as[23]

$$r_{33} = 3r_{13} = -\frac{8\pi f N \beta}{{n_0}^4}\left(\frac{1}{3}p - \frac{1}{45}p^3 + \frac{2}{945}p^5 - \frac{2}{9450}p^7 + \ldots\right) \quad (1)$$

where N is the number density of the NLO chromophore molecules, β the molecular first hyperpolarizability, n_0 the refractive index, f an appropriate local field factor, and $p = \mu_d E/kT$ with μ_d being the molecular dipole moment, E the applied electric field, k the Boltzman constant, and T the absolute temperature. The solid curve in Figure 4 shows a fit of the experimental data to eq 1. It should be pointed out that the EO coefficients reported in this paper contain contributions from the field induced birefringence due to the low T_g of the material. More accurate measurements of EO coefficients can be performed at high modulation frequencies at which the chromophores can only partially respond to the ac component of the applied field and, thus, contribution from birefringence be minimized.[24]

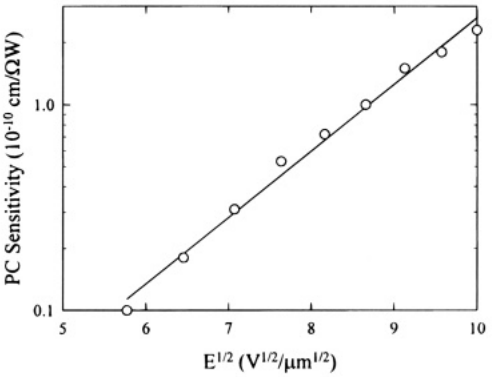

Figure 5. Electric field dependence of the photoconductivity (PC) sensitivity.

The photoconductivity (σ) and the photoconductivity sensitivity (S) of the material are calculated using the experimentally measured photocurrent (I_{ph}) flowing through the film using[25]

$$\sigma = \frac{L}{AV/I_{ph}} \qquad S = \sigma/I_0 \quad (2)$$

respectively. Here L is the sample thickness, A the illumination area (the same as the gold electrode area), V the applied dc voltage, and I_0 the illumination laser power density. Figure 5 displays an electric field dependence of the photoconductivity sensitivity. The photoconductivity sensitivity is plotted against the square root of the applied dc electric field on a semilog scale. A linear dependence has been obtained for fields between 30 and 100 V/μm.

B. Photorefractive Properties. Photorefractivity is a combined effect of the electrooptic response and photoconductivity simultaneously present in the material. The illumination of two coherent laser beams creates an interference pattern with bright and dark regions. The photocharges generated in the bright regions migrate to dark regions and become trapped, creating a space charge field with an amplitude (E_{SC}) given by[1,2]

$${E_{SC}}^2 = \frac{{E_D}^2 + {E_{0G}}^2}{(1 + E_D/E_q)^2 + (E_D/E_q)^2(E_{0G}/E_d)^2} \quad (3)$$

where E_{0G} is the component of the applied field, E_0, along the space charge grating wavevector. The drift

(23) Prasad, P. N.; Williams, D. J. *Introduction to Nonlinear Optical Effects in Polymers and Molecules*; Wiley: New York, 1991.

(24) Moerner, W. E.; Silence, S. M.; Hache, F.; Bjorklund, G. C. *J. Opt. Soc. Am. B* **1994**, *11*, 320.

(25) Zhang, Y.; Spencer, C. A.; Ghosal, S.; Casstevens, M. K.; Burzynski, R. *J. Appl. Phys.* **1994**, *76*, 671.

field E_D and the limiting space charge field E_q are defined as

$$E_D = \frac{K_G kT}{e} \qquad E_q = \frac{eN_T(N_S - N_T)}{\epsilon\epsilon_0 K_G N_S} \tag{4}$$

respectively, where N_S is the number density of the photocharge sensitizing molecules, N_T is the number density of traps, K_G is the space charge field wavevector, ϵ is the dielectric constant of the composite and ϵ_0 is the vacuum permittivity. The space charge field is phase shifted with respect to the interference pattern by a value φ given by

$$\tan\varphi = \frac{E_D}{E_0}\left(1 + \frac{E_D}{E_q} + \frac{E_0^2}{E_D E_q}\right) \tag{5}$$

This phase shift can be measured in a two-beam coupling experiment by translating the gratings in the direction of the grating wavevector in a time shorter than that required to build the gratings. The space charge field modulates the refractive index of the material through the electrooptic effect to form a refractive index grating with

$$\Delta n = -\,{}^1/_2 n_0^3 r E_{SC} \tag{6}$$

where r is the electrooptic coefficient. This refractive index grating can be detected by a reading beam which is diffracted by the grating with diffraction efficiencies given by[26]

$$\eta_s = \sin^2\left(\frac{\pi n^3 r_{13} E_{SC} L \sin\theta_G}{2\lambda(\cos\theta_1 \cos\theta_2)^{1/2}}\right)$$

$$\eta_p = \sin^2\left(\frac{\pi n^3 r_{eff}^p E_{SC} L \cos 2\theta_0}{2\lambda(\cos\theta_1 \cos\theta_2)^{1/2}}\right) \tag{7}$$

for s- and p-polarized reading beams, respectively. In eq 7, θ_1 and θ_2 are the incidence angles of beams 1 and 2, respectively, and θ_0 the full angle between the writing beams, all inside the material. The effective electrooptic coefficient r_{eff}^p in eq 7 is given by

$$r_{eff}^p = r_{13}[\cos\theta_1 \sin(\theta_2 + \theta_G) + \sin\theta_1 \cos\theta_2 \cos\theta_G] + r_{33} \sin\theta_1 \sin\theta_2 \sin\theta_G \tag{8}$$

where θ_G is the angle between the index grating wavevector and the sample surface plane.

Figure 6 presents the electric field dependence of the photorefractive four-wave mixing diffraction efficiency obtained in the material. This field dependence is typical of low-T_g materials since the electrooptic coefficient and the space charge field are both electric field dependent as shown by eqs 1 and 3. The experimentally measured data were fitted to eq 7 and the solid line in Figure 6 shows such a fit.

According to the band model transport theory, the buildup of a photorefractive index grating can be described by

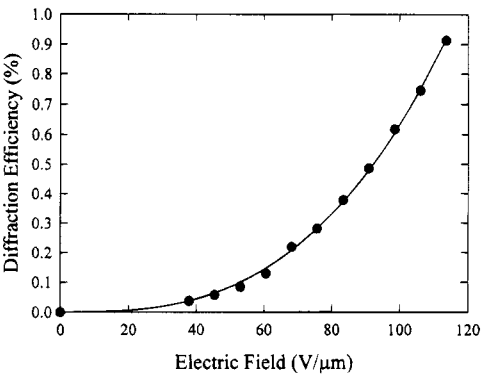

Figure 6. Electric field dependence of the four-wave mixing diffraction efficiency. Filled circles: experimental data; solid curve: fit to eq 7.

$$E_{SC} = E_{SC}^0[1 - \exp(-t/\tau_e)] \tag{9}$$

where E_{SC}^0 is the saturation space charge field and τ_e is the space charge field buildup time constant which is proportional to the material's dielectric relaxation time, τ_{di}, given by

$$\tau_e = a\tau_{di} \qquad \tau_{di} = \frac{\epsilon}{4\pi e\mu N_0} \tag{10}$$

provided that the recombination time is much shorter than the dielectric relaxation time. In eq 10, a is a proportional constant, μ is the photocharge mobility, and N_0 is the number density of charge carriers.

When the space charge grating is uniformly illuminated by a laser beam, it is erased due to the charge redistribution in the material through diffusion and drift. The decay of the space charge field typically takes the form of

$$E_{SC} = E_{SC}^0 \exp(-t/\tau_{er}) \tag{11}$$

with $\tau_{er} = \tau_e$, and the erasure process has the same time constant as the writing process.

The inset of Figure 7 shows a typical four-wave mixing signal obtained from the present polymer material. The writing and erasure processes are fitted to eqs 9 and 11, respectively. The holographic grating formation and erasure dynamics were studied by measuring the writing and erasure time constants and their electric field dependence, and the results are presented in Figure 7. In this figure, the writing rate is plotted against the square root of the applied electric field. This field dependence of the writing rate can be explained by the field dependence of the charge mobilities, expressed as[27]

$$\mu(E,T) = \mu_0 \exp\{-T_0^2/T^2 + E^{1/2}(\theta/T^2 - \gamma)\} \tag{12}$$

where T is the temperature in kelvin and T_0, θ, and γ are the experimentally determined constants for a particular material. Therefore, the writing rate shows a field dependence of $\tau^{-1} \propto \exp(E^{1/2})$ or $\log(\tau^{-1}) \propto E^{1/2}$. This is indeed our observation as evidenced by the experimental data shown in Figure 7.

(26) Kogelnik, H. *Bell Sys. Technol. J.* **1969**, *48*, 2909.

(27) See, for example: Gill, W. D. Polymeric photoconductors. In *Photoconductivity and Related Phenomena*; Mort, J., Pai, D. M., Eds.; Elsevier: New York, 1976.

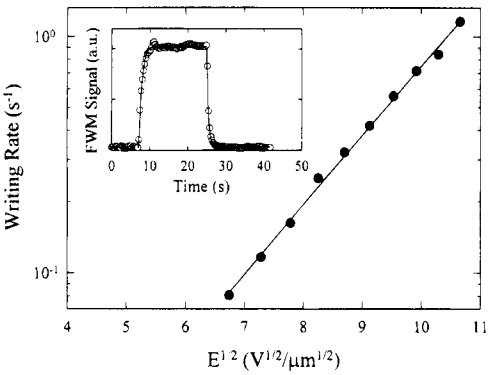

Figure 7. Electric field dependence of the writing rate. The inverse of the writing time constant is plotted against the square root of the applied electric field. Inset: a typical four-wave mixing (FWM) signal. Open circles: experimental data. The writing process is fitted to eq 9 and the erasure process fitted to eq 11.

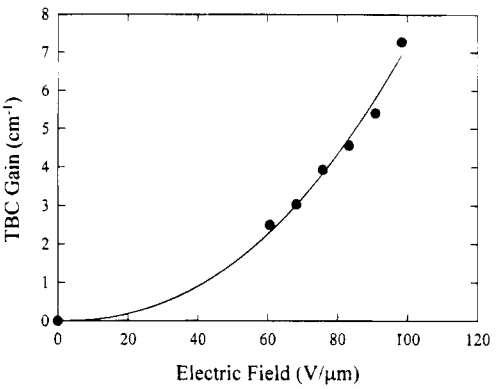

Figure 8. Electric field dependence of the two-beam coupling (TBC) gain.

The most important feature of the photorefractive effect, which distinguishes itself from many other mechanisms that may result in refractive index gratings, is the finite phase shift between the refractive index grating and the interference pattern, as described by eq 5. This finite phase shift, or the nonlocal nature of the photorefractive effect, causes an asymmetric energy transfer between the writing beams, a unique process which does not occur in any of the other processes. Therefore, the photorefractive nature of the composite can be further confirmed by the asymmetric energy transfer in two-beam coupling experiments. First, the intensities of the writing beams were monitored as the electric field was turned on and off. An energy transfer is evidenced by the increase in the intensity of beam 1 and decrease in that of beam 2. When the electric field was turned off, no intensity changes were observed. Two more experiments were carried out in order to observe the growth of the space charge gratings in the presence of the applied field. The intensity of beam 1 was monitored while beam 2 was open and then blocked and the same experiment was repeated for beam 2. The two-beam coupling gain is calculated using the following equation:

$$\Gamma = \frac{1}{L/\cos\theta}[\ln(\gamma_0\xi) - \ln(\xi + 1 - \gamma_0)] \qquad (13)$$

where L is the sample thickness, ξ is the ratio of the beam intensities, $\gamma_0 = P/P_0$ is the beam coupling ratio where P_0 is the detected signal without the pump beam and P is the signal with the pump beam on, and $\theta = \theta_1$ or θ_2 is the incidence angle of the beam inside the material. The two-beam coupling gain was measured as a function of the electric field, and the dependence is shown in Figure 8. It is worthy pointing out that the material did not show a net two-beam coupling gain since the gain does not exceed the absorption coefficient (25 cm^{-1}) at the operation wavelength.

IV. Discussion and Conclusion

The polymer presented in this paper possesses charge-transporting and electrooptic properties arising from the carbazole group and the second-order NLO chromophore, respectively, both covalently attached to the polymer backbone. When doped with a photocharge generation sensitizer, photorefractivity has been observed. Problems associated with phase separation are clearly avoided because of the covalent bonding and of the low concentration of the photocharge generation sensitizer. However, the observed photorefractive properties do not seem to compare favorably with that obtained from composite (or guest–host) materials, in terms of the four-wave mixing diffraction efficiency, two-beam coupling gain, and the holographic grating writing dynamics.

The holographic grating formation dynamics is directly related to the photoconductivity (or charge mobility) of the material. As the results show, the grating writing time constant at a power level of 250 mW/cm^2 and an electric field of 100 V/μm is around 0.5 s. The overall grating writing speed is slower than that reported for composite materials (as short as 60 ms).[15,25] This may be a result of the low charge mobilities in polymers where the charge-transporting agent and second-order chromophores are covalently bound to the polymer backbone, as has been observed in other fully functional photorefractive polymers.[13,14] Compared with guest–host systems, the molecular motions of the charge-transporting agents in fully functional polymers are restricted to very short-range vibrations and rotations at temperatures below the glass transition temperature (T_g). This restricted molecular motion may thus interrupt the conduction pathway of the charge-transporting molecules, resulting in slower photorefractive responses.

In summary, a new low-T_g photorefractive polymer has been synthesized and characterized which contains a hole-transporting group, a nonlinear optical chromophore, and a long aliphatic n-octyl methacrylate group to lower the polymer's glass transition temperature. The experimental results demonstrated that the major contribution to the photorefractive effect comes from the space charge field due to the light-induced charge separation with a subsequent effective electric-field-induced refractive index change.

Acknowledgment. The authors gratefully acknowledge support of this work by the Air Force Office of Scientific Research through Contract Numbers F49620-93-C-0017 (SUNY at Buffalo) and F49620-92-C-0061 (LPT, Inc.).

CM950025A